PEER-TO-PEER LOW ANTENNA OUTDOOR RADIO WAVE PROPAGATION AT 1.8 GHZ

Neal Patwari, Gregory D. Durgin, Theodore S. Rappaport, Robert J. Boyle

Mobile & Portable Radio Research Group
Bradley Department of Electrical and Computer Engineering
Virginia Polytechnic Institute and State University
Blacksburg, VA 24061-0111 Tel: (540)231-2927 Fax: (540)231-2968
e-mail: wireless@vt.edu

Abstract – In this outdoor propagation study, low antenna heights of 1.7 m are used at both the transmitter and the receiver to measure wideband (100 MHz baseband) power-delay profiles (PDPs) of the channel for a peer-to-peer communications system operating at 1.8 GHz. Rural and urban areas are studied in 22 different transmitter-receiver links, and the path loss and delay spread characteristics are presented. The small-scale multipath fading characteristics are measured in detail by recording 160 PDPs within each local area. This paper shows the measurement setup for calculation of the fading rate variance and the estimation of the angular spread of each multipath component. The accuracy of the angular spread is discussed.

I. Introduction

A *peer-to-peer* communications system operates without a base station. Mobile or portable units operate directly with one another. Users will be sitting in a vehicle or standing while using their mobile unit and, as a result, the antenna heights are between one and two meters high for both transmitter and receiver. Due to the very low antenna heights, it is a different propagation environment than previously considered for microcellular systems, which operate with higher base station antennas (5 to 15 m). New propagation measurements are required to understand the channel characteristics.

The measurements reported here show the time-dispersion and the small-scale fading characteristics of the multipath channel. Accurate modeling of both are necessary for the design of wideband and high bit rate mobile-to-mobile communication systems.

*This material is based upon work supported under a National Science Foundation Graduate Fellowship and Presidential Faculty Fellowship, and a Bradley Fellowship in Electrical Engineering.

II. Measurement Setup

The transmitter and receiver block diagrams of the spread spectrum channel sounder used in this measurement campaign are shown in Fig. (1). The PN sequence generator is run at 100 MHz (chip period $T_c = 10$ ns) using a sequence length of 2047. The slip rate is $f_s = 10$ kHz, and the time scale factor is $\gamma = 10^4$ [1]. The null-to-null RF bandwidth of the system is 200 MHz at a carrier frequency of 1.8 GHz. Both the transmitter and receiver use 4 dBi bicone antennas which have their maximum gain along the azimuth and a 3 dB vertical beamwidth of 30^o. These antennas are wideband such that the gain pattern and impedance are constant over the 200 MHz bandwidth.

The estimation of the fading rate variance (the mean-square rate of power change in a local area) requires measurements along two linear and perpendicular tracks. Thus in each local area, the receiver antenna is moved along two perpendicular tracks each of length 20λ. Measurements are taken every $\lambda/4$. We are interested in the small-scale fading characteristics, not the fading due to temporal variations in the channel. Thus the effects of channel transients are undesirable. Ten PDP waveforms are captured at each position along the track and averaged together to help reduce the effect of channel transients such as moving cars, people, and leaves.

III. Analysis and Results

Power-Delay Profiles

The MPRG sliding correlator measurement system has been reported in [1]. Consider the channel to be a linear filter given by $h(t) = \sum_{i=1}^{K} \alpha_i e^{j\phi_i} \delta(t - \tau_i)$, where α_i, ϕ_i, and τ_i, are the amplitude, phase, and

0-7803-5565-2/99/$10.00 © 1999 IEEE

time delay of the ith multipath component. Taking into account the change in phase due to change in receiver position $\vec{r}$, the output of the measurement system, the power-delay profile, is

$$P(\tau, \vec{r}) = \left| \sum_{i=1}^{K} \alpha_i e^{j(\phi_i + \vec{k}_i \cdot \vec{r})} R_p(\tau - \tau_i) \right|^2 \qquad (1)$$

where $R_p(\tau)$ is the autocorrelation of the pseudo-noise (PN) signal. $R_p(\tau)$ is almost zero except for a triangular peak between $-T_c < \tau < T_c$. The wave and position vectors are given by $\vec{k}_i$ and $\vec{r}$, respectively, where the direction of $\vec{k}_i$ is the angle-of-arrival (AOA) of the ith multipath component and the magnitude is $2\pi/\lambda$.

Eq. (1) is important because it shows that the power-delay profile is the magnitude squared phasor sum of K autocorrelation functions. If we neglect the small $(-1/N)$ correlation in-between the peaks, then $x(\tau)$ has overlapping correlation peaks when multipath delays, τ_i, are closer than $2 * T_c$ to each other.

At each of the 22 receiver locations, the 160 PDPs taken within the local area are averaged to form the spatial average PDP. An example spatial average PDP is shown in Fig. (2).

Narrowband Path loss

Total received power can be computed from the linear spatial average PDP simply by summing the powers of the multipath components [2]. In the path loss exponent model, the mean total path loss at a distance d is given simply by

$$\bar{PL}_{nb}(d) = PL_{ref}(d_0) + 10n log_{10} \frac{d}{d_0} \qquad (2)$$

where $PL_{ref}(d_0)$ is the reference path loss calculated by assuming free-space propagation until the reference distance d_0 [2]. This model is a measurement-based model, where d_0 is chosen and n is determined from least-squared error analysis. Calculation of the path loss exponent, shown in Fig. (3), results in $n = 2.8$ and $d_0 = 5$ m. A previous propagation study at 1.9 GHz on the Virginia Tech campus with the same antenna heights as in this study found $n = 2.7$ [3], which lends confidence to these results.

RMS Delay Spread

In wideband radio design the RMS delay spread, σ_τ, gives insight into the coherence bandwidth of the

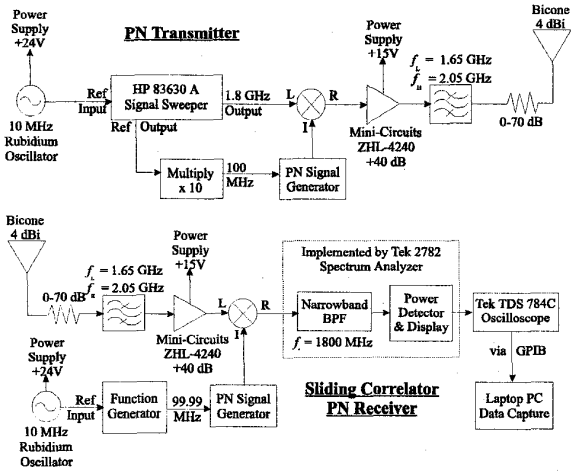

Figure 1: Block diagram of the transmitter and receiver.

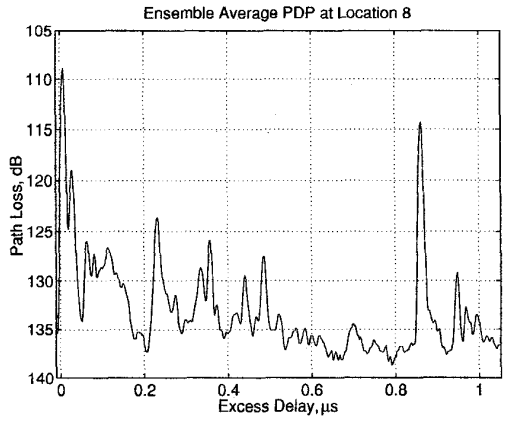

Figure 2: Beef Cattle Farm link, a rural env. OBS by terrain, $d = 332$m, $\bar{P}_{nb} = 106.2$ (dB).

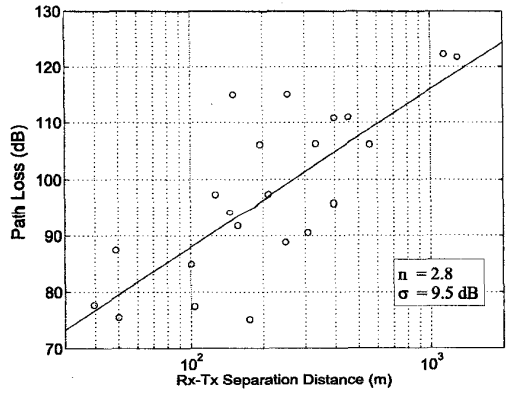

Figure 3: The path loss measurements and path loss exponent model.

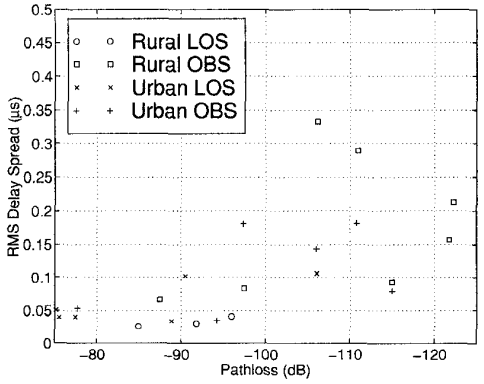

Figure 4: Measured RMS delay spreads grouped by environment type.

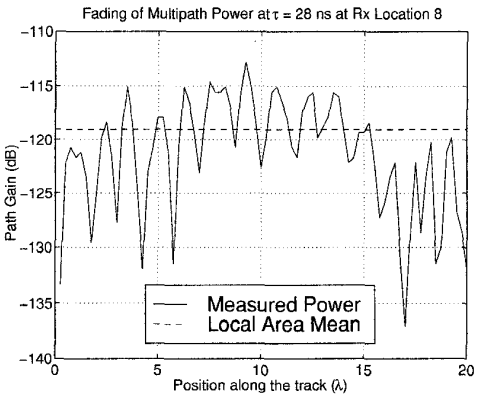

Figure 5: Measured power along a linear track of the peak at $\tau = 28$ ns in the PDP shown in Fig. (2). The calculated $\Lambda^2 = 0.35$.

channel. The RMS delay spreads, calculated from each of the 22 spatial average PDPs, are shown in Fig. (4). As found in [4], the RMS delay spreads show an *exponential overbound*, that is, maximum RMS delay spreads increase exponentially with path loss but the minimum remains almost constant.

Wideband Fading Rate Variance

In a small local area, we assume that the amplitudes of the multipath waves are approximately constant while the phases vary as a function of receiver position and AOA of the incoming waves. If a peak on the PDP is a result of more than one multipath within $2 * T_c$ of each other, then the peak undergoes small-scale fading as the receiver antenna moves along the track. A measured track example is shown in Fig. (5). If the fading waveform of the PDP peak is expressed as $P_n(\tau, x)$, where τ is the time delay of the peak and x is the position along the track at receiver location n, then the fading rate variance is

$$\sigma_x^2 = E\left[\left(\frac{dP}{dx}\right)^2\right]. \tag{3}$$

The slope of a sampled signal is calculated by supersampling the measured waveform at rate R. That is, it is first padded with zeros and fast Fourier transformed. Next it is filtered to the limiting bandwidth and inverse fast Fourier transformed. The original waveform has 80 samples, and after this supersampling with rate R, the new waveform is $80R$ in length. The slope of the supersampled power waveform, $\dot{P}_n(\tau, x)$ at position x_i is approximately $\frac{\dot{P}_n(\tau,x_{i+1}) - \dot{P}_n(\tau,x_i)}{\Delta x}$. Thus the estimated fading rate variance along the x track is calculated using:

$$\hat{\sigma_x^2} = \frac{1}{80R-1} \sum_{i=1}^{80R-1} \left[\frac{\dot{P}_n(\tau, x_{i+1}) - \dot{P}_n(\tau, x_i)}{\lambda/(4R)}\right]^2. \tag{4}$$

As the supersampling rate R is made high (≥ 10), the approximation error becomes very low.

Durgin [5, 6] has shown that measured fading rate variances along two perpendicular tracks can be used to estimate the fading rate variance in an arbitrary direction. If σ_x^2 and σ_y^2 are the fading rate variances along the x and y axis, then the mean for a receiver moving in an arbitrary direction is given by

$$\sigma_S^2 = \frac{1}{2}\left(\sigma_x^2 + \sigma_y^2\right). \tag{5}$$

Durgin showed the angular spread, Λ^2, of the incoming multipath waves is directly proportional to this mean fading rate variance,

$$\Lambda^2 = \frac{4\pi^2}{\lambda^2}\sigma_S^2. \tag{6}$$

In this paper we plot the angular spread computed from Eq. (6). However, consideration of the mean fading rate variance can be done by scaling the result. The angular spread and PDP at 8 typical receiver locations are plotted in Fig. (6) for the urban locations and in Fig. (7) for the rural locations.

IV. Discussion

Observe in Figs. (6) and (7) the behavior of angular spread, Λ^2, as a function of τ. Note that a classical Jakes omnidirectional AOA pattern for a single multipath component results in $\Lambda^2 = 1$ [5]. We see

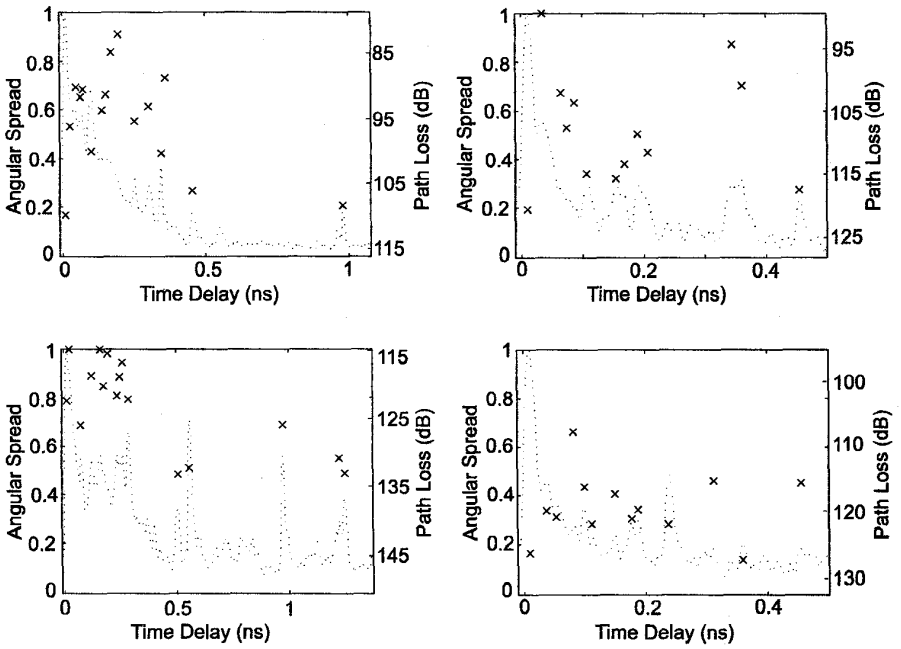

Figure 6: Measured angular spread and spatial average PDP at 4 urban locations.

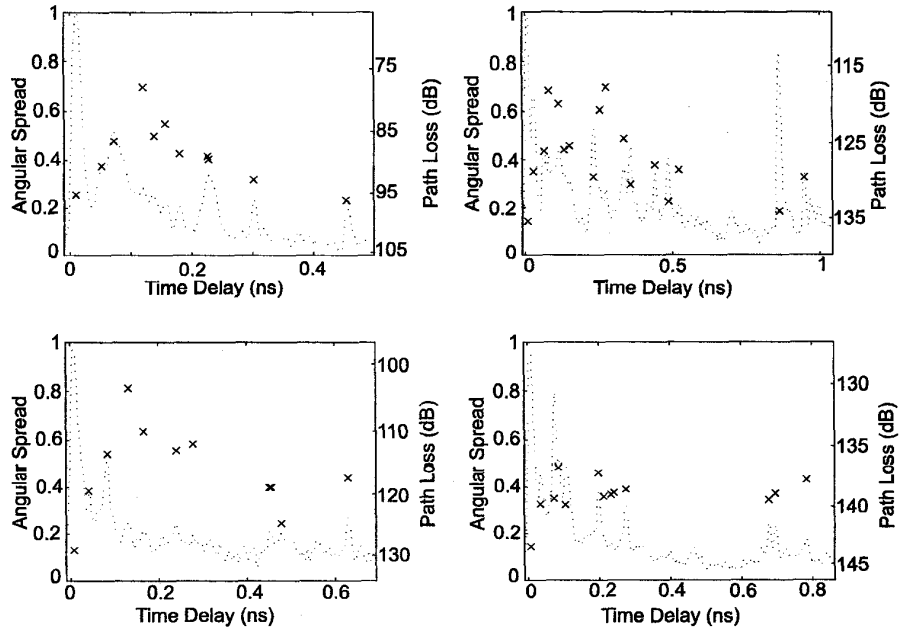

Figure 7: Measured angular spread and spatial average PDP at 4 rural locations.

that the first PDP peak (especially in an LOS link) usually has a very low Λ^2. This is because the only multipath power that can lead to a non-zero angular spread comes from scatterers within a very narrow ellipse with foci at the receiver and transmitter [7]. The measurements also show that Λ^2 rises quickly for low τ. This is due to the likelihood that at low τ many multipath components contribute to the PDP peaks. In addition, as τ increases, the ellipse of possible scatterers becomes more circular. It is apparent that received power is more likely to be spread out all around the receiver. However, at large τ, the measured Λ^2 falls again. We expect this since multipath arrive infrequently at long delays, and individual multipath are likely to be resolvable by the measurement system.

The measured Λ^2 never goes to zero, however, and this may be due to one of three effects. First, we expect that the operator and his measurement equipment served as unwitting scatterers, artificially increasing the angular spread (and thus the fading rate variance) at the receiver. Second, the transients in the channel such as moving cars, people, tree branches and leaves, contribute to the fading. Even though 10 PDPs were averaged at each position along the track to mitigate the effects of the channel transients, they still had an effect. Finally, for very low PDP power peaks, additive noise contributes to the variations in the fading waveform.

Note that very high Λ^2 values usually correspond to relatively low power PDP peaks. This may attest that there is not a strong multipath component dominating the power contributing to that peak.

Angular spread is higher on average in urban areas than in rural areas. The higher density of scatterers in urban environments is likely the cause.

V. Conclusion

These wideband measurements are unique, both for their use of very low antenna heights at the transmitter and receiver, and for their application to new theory relating fading rate variance and angular spread.

The reported path loss and RMS delay spreads are useful for design of peer-to-peer devices in either rural or urban environments. RMS delay spreads of up to 330 ns in rural and up to 200 ns in urban peer-to-peer environments were found. A pathloss exponent of 2.8 is the best fit to experimental data.

The expected characteristics of angular spread (or fading rate variance) as a function of time delay and environment type are met. Designers of rake receivers must consider that at low time delays and at low power levels, the received power in a rake finger is likely to experience the highest degree of envelope fading. However, the multipath at long time delays should experience much less fading and may make better sources of multipath diversity for a rake receiver. The results suggest the validity of Durgin's work in [5, 6], that angular spread characteristics can be calculated by measuring received power along two linear and perpendicular tracks.

References

(1) W. Newhall, T. Rappaport, and D. Sweeney, "A Spread Spectrum Sliding Correlator System for Propagation Measurements," *RF Design*, pp. 40–54, April 1996.

(2) T. Rappaport, *Wireless Communications: Principles and Practice.* New Jersey: Prentice-Hall Inc., 1996.

(3) K. Saldanha and J. Reed, "Performance Evaluation of DECT in Different Radio Environments," Tech. Rep. MPRG-TR-96-28 (163 pages), Virginia Tech, http://scholar.lib.vt.edu/theses/index.html, Aug 1996.

(4) M. Feuerstein, K. Blackard, T. Rappaport, S. Seidel, and H. Xia, "Path Loss, Delay Spread, and Outage Models as Functions of Antenna Height for Microcellular System Design," *IEEE Transactions on Antennas and Propagation*, vol. 43, pp. 487–498, Aug 1994.

(5) G. Durgin and T. Rappaport, "A Basic Relationship Between Multipath Angular Spread and Narrowband Fading in a Wireless Channel," *IEE Electronics Letters*, vol. 34, pp. 2431–2432, 10 Dec 1998.

(6) G. Durgin and T. Rappaport, "Effects of Multipath Angular Spread on the Spatial Cross-Correlation of Received Voltage Envelopes," in *IEEE 49th Vehicular Technology Conference*, (Houston TX), May 1999.

(7) J. Liberti and T. Rappaport, "A Geometrically Based Model for Line-of-sight Multipath Radio Channels," in *IEEE 46th Vehicular Technology Conference*, (Atlanta GA), pp. 844–848, April 1996.